



Simulated reflection spectra of copper red glaze and gold ruby-pink enamel

Gen Li^a , Cui Jia, Baoqiang Kang, He Li, Yong Lei^b

Department of Conservation Science, The Palace Museum, Beijing 100009, People's Republic of China

Received: 12 November 2024 / Accepted: 29 March 2025

© The Author(s), under exclusive licence to Società Italiana di Fisica and Springer-Verlag GmbH Germany, part of Springer Nature 2025

Abstract Copper red glaze and gold ruby-pink enamel are two typical ancient red glazes with high artistic value. At present, researchers already have a good knowledge of copper red glaze, but due to the scarcity of samples, people's understanding of gold ruby-pink enamel is still insufficient and mostly stays at the qualitative level. Based on the multiple scattering theory, we have previously established a framework to calculate the reflection spectra of such colloidal colored glazes and proved that metallic copper nanoparticles are the main colorants of copper red glazes. In this paper, we used this model to systematically study the reflection spectra of copper red glaze and gold ruby-pink enamel under different particle diameters, volume fractions, glaze thickness, and refractive indices of glaze and discussed the relationship between these parameters and the observed glaze color. Then, starting from the basis of Mie scattering theory, the difference in the optical properties of these two red glazes is clearly explained by calculating the scattering coefficients and absorption coefficients of nanoparticles with different particle sizes.

1 Introduction

As a typical representative of Chinese cultural heritage, ancient ceramics have been one of the cultural symbols of China from ancient to the present and have received broad attention from researchers at home and abroad. Ancient ceramics provide us with a glimpse into the flourishing trade and cultural exchanges between China and foreign countries in ancient times, and their rich and colorful glaze effects are a reflection of the exquisite skills of ancient craftsmen, which have always been praised by the world.

Existing studies generally believe that, on the one hand, the glaze color of ceramics is related to the chemical state of different transition metal ions; while on the other hand, the microstructures in the glaze, such as unmelted raw materials, crystals and bubbles generated during the firing process, will also affect the color rendering effect of the glaze, especially the second-phase particles often play a crucial role in the color performance of many ancient ceramics [1–3]. Moreover, even for the same kind of second-phase particles, when the particle size, volume fraction, and distribution mode change, the effect of the glaze will also be significantly different.

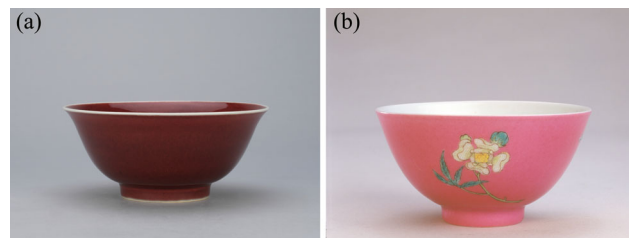
In order to quantitatively analyze the relationship between the second-phase particles in the glaze and the presented color, we have previously established a two-channel numerical model based on multiple scattering theory, and it was applied to the research of copper red glaze [4]. In order to find out whether the source of the red color of the ancient copper red glaze is the metallic copper nanoparticles or cuprous oxide nanoparticles, we simulated the reflection spectra of the two nanoparticles with different particle diameters and different volume fractions in the transparent glaze and found that the metallic copper particles may make the glaze appear as a good copper red glaze in the range of 20–200 nm, but the required volume fraction is different when the particle diameter is different. When cuprous oxide nanoparticles are used as scatterers, the spectral characteristics are significantly different from those produced by metallic copper particles, and the results of our analysis of copper red samples with TEM also support our calculations, thus answering the question that has puzzled the academic community for more than 30 years. The bowl with bright red glazed shown in Fig. 1a, which was produced during the Xuande reign period, Ming Dynasty, is a representative object of copper red glaze.

Later, one article published in *Heritage* studied Roman glass tesserae from the fourth century A.D. and found that orange glass samples were mainly colored by cuprous oxide; [5] while another article on Spanish red glass reported that the red color was derived from Cu⁰ particles. [6] These analysis results once again justify our calculations.

However, we note that an important parameter in Mie scattering theory is the relative refractive index, i.e., the ratio of the refractive index of the second-phase particle to the matrix [7], so theoretically, the reflection spectrum of the transparent glaze should be different when the refractive index is different. It is a well-known fact that diamonds shine because of their high refractive index (about 2.4). And we know that with the different glaze formulations, the refractive index of ancient porcelain enamel can vary

^ae-mail: g-li14@tsinghua.org.cn (corresponding author)

Fig. 1 **a** Bowl with bright red glazed bowl, which was produced during the Xuande reign period, Ming Dynasty; **b** Bowl with famille rose decoration and butterfly pattern, which was produced during the Yongzheng reign period, Qing Dynasty. (courtesy of the Palace Museum)



in the range of about 1.4–1.8, so what kind of color will be produced in glazes with different refractive indices by the same copper nanoparticles, has become a rather interesting question.

On the other hand, among the many ancient porcelain enamels, the famous gold ruby-pink enamel, which was introduced to China during the Kangxi reign of the Qing Dynasty, is also a glaze similar to the copper red glaze that used metal nanoparticles to manifest the color [8, 9]. As a kind of low-temperature glaze that appeared lately, the appearance of gold ruby-pink has brought a new choice to the creation of colored porcelain, and greatly enhanced the artistic expression of famille rose and color enamels. The gold nanoparticles can even produce iridescent effects under specific arrangements [10]. The bowl with famille rose decoration and butterfly pattern shown in Fig. 1b, which was produced during the Yongzheng reign period, Qing Dynasty, is a typical representative of gold ruby-pink enamel.

At present, the consensus on gold ruby-pink enamel is that its color is derived from gold nanoparticles, which usually appears as peach red or pink; it contains a certain amount of lead oxide, has a high refractive index, and belongs to low-temperature glaze. However, due to the scarcity of samples, the understanding of gold ruby-pink enamel is still in the qualitative level and much less sufficient than copper red glaze. For example, some researchers claim that the gold ruby-pink enamel can achieve good appearance when the diameters of gold nanoparticles are in the range of 20–80 nm [9]; some researchers have tested commercial gold ruby-pink pigments and found that the particle diameters are mainly concentrated in the range of 10–25 nm [11]; simulation experiments have also been conducted to study the changes in the diameters of gold nanoparticles under oxidative and reducing atmosphere firing [12]. However, few people can answer the questions at the quantitative level: how the color of the glaze changes when the size and content of gold nanoparticles change, and at what size and content can the most perfect gold ruby-pink enamel be obtained.

Previous literature and our experiments have confirmed the existence of a "transparent-red-transparent" sandwich-like glaze layer structure in copper red glaze [4, 13], but few people have systematically studied the body and glaze structure of gold ruby-pink enamel products. Intuitively, the thickness of the colored layer will definitely affect the color of the enamel, but the direct relationship between the glaze color and the thickness is not clear enough and still requires more quantitative analysis and discussion.

In view of this, this paper will simulate the reflection spectra of copper red glaze and gold ruby-pink enamel under different conditions on the basis of previously established model, analyze the relationship between particle diameter, volume fraction, glaze thickness, glaze refractive index and other parameters and color, then compare the similarities and differences between these two red glazes, and provide a new perspective for the coloration problems of ancient ceramic glaze.

2 Method

2.1 Computational frame

Here we only briefly introduce the idea of using our model to calculate reflection spectra. For more details, please refer to our work [4] and previous references [14–16].

2.1.1 Interaction cross section of one single particle for light

In our computational simulation, at the core is the interaction cross section of the second-phase particles for light in the glaze. Define $\sigma_{\text{abs}}(\lambda, d)$, $\sigma_{\text{sca}}(\lambda, d)$ and $\sigma_{\text{ext}}(\lambda, d) = \sigma_{\text{abs}}(\lambda, d) + \sigma_{\text{sca}}(\lambda, d)$ to be the absorption, scattering and extinction cross section, respectively, of a single particle with diameter d relative to the light of wavelength λ , and they are the functions of λ and d . These cross sections can be written as the product between corresponding dimensionless coefficients and the projection areas of these particles, namely $\sigma_{\text{abs}}(\lambda, d) = Q_{\text{abs}}(\lambda, d) \times \pi d^2 / 4$, $\sigma_{\text{sca}}(\lambda, d) = Q_{\text{sca}}(\lambda, d) \times \pi d^2 / 4$ and $\sigma_{\text{ext}}(\lambda, d) = Q_{\text{abs}}(\lambda, d) + Q_{\text{sca}}(\lambda, d)$.

For a given wavelength λ and diameter d , these three dimensionless coefficients $Q_{\text{abs}}(\lambda, d)$, $Q_{\text{sca}}(\lambda, d)$ and $Q_{\text{ext}}(\lambda, d)$ can be calculated by Mie scattering theory [16], and they are related to the complex refractive index of both the particle and the transparent glaze. In our calculation, the refractive indices of gold and copper are from reference [18].

For simplicity, in our system the scattering light is simplified as forward scattering and backward scattering, and the forward/backward ratio r_{fb} is defined as the ratio of the power of forward and backward light scattered by a spherical particle. It can be calculated by integrating the power of scattered light under different scattering angles.

2.1.2 The interaction of one single thin layer with light

Under the assumption that the particles are uniformly dispersed in the horizontal plane (not necessary to be uniformly dispersed along depth direction), we can divide the glaze layer into N thin layers along the depth direction. Define t as the thickness of each layer, and s as the transmittance of this thin layer of glaze. Then we will discuss the interaction of this thin layer of glaze with light.

Define the volume fraction of copper-containing particles in the glaze as ω , then the particle number in per unit volume (namely the number density) is $\rho = 6\omega/\pi d^3$. Denote $C_a(\lambda, d) = \rho\sigma_{abs}$, $C_s(\lambda, d) = \rho\sigma_{sca}$, they stand for the absorption and scattering intensity of the glaze with unit thickness.

If the intensity of incident light is I_0 , the absorbed intensity is $I_{abs} = I_0[1 - \exp(-tC_a(\lambda, d))]$, and the scattered intensity (forward + backward) is $I_{sca} = I_0[1 - \exp(-tC_s(\lambda, d))]$.

After the incident light interacts with this thin layer, the light intensity I_f along the original direction, and light intensity I_b along the backward direction are

$$\begin{cases} I_f = (I_0 - I_{abs} - I_{sca})s + I_{sca}\frac{r_{fb}}{1+r_{fb}} = C_{ff}(\lambda, d, t)I_0 \\ I_b = I_{sca}\frac{1}{1+r_{fb}} = C_{bb}(\lambda, d, t)I_0 \end{cases}$$

here

$$\begin{cases} C_{ff}(\lambda, d, t) = s[\exp(-tC_a(\lambda, d)) + \exp(-tC_s(\lambda, d)) - 1] + \frac{r_{fb}[1-\exp(-tC_s(\lambda, d))]}{1+r_{fb}} \\ C_{bb}(\lambda, d, t) = \frac{[1-\exp(-tC_s(\lambda, d))]}{r_{fb}+1} \end{cases}$$

2.1.3 The interaction of multi layers of glaze with light

For the thin layer numbered as i , if we define I_i as the intensity of the incident light into the upper surface, O_i as the intensity of the outgoing light away from the upper surface, then the outgoing light O_{i+1} away from the upper surface of thin layer $i+1$ will be the incident light into the lower surface of thin layer i , and the incident light I_{i+1} into the upper surface of thin layer $i+1$ is also the outgoing light away from the lower surface of thin layer i .

Based on relationships above, the outgoing light intensity away from the thin layer i can be written as:

$$O_i = C_{bb}(\lambda, d, t)I_i + C_{ff}(\lambda, d, t)O_{i+1}$$

And the outgoing light intensity away from the lower surface of thin layer i can be written as:

$$I_{i+1} = C_{ff}(\lambda, d, t)I_i + C_{bb}(\lambda, d, t)O_{i+1}$$

The above two formulas are the relationships that light should satisfy when propagating inside the glaze. After taking into consideration the boundary condition, namely the reflectivity r_1 at the glaze-air interface, and the reflectivity r_2 at the body-glaze interface, the light intensity at various locations in the system can be fully calculated, including the intensity of light emitted from the glaze surface to the air. The ratio of this intensity to the incident intensity is the reflectivity of the system to light of wavelength λ . The reflectivity r_1 can be calculated by Fresnel formula, the reflectivity r_2 can be estimated by the whiteness of the body. After calculating the emitted intensity of different wavelengths of light, the reflection spectrum of the transparent glaze model can be obtained.

2.2 Estimation of the refractive index of the glaze

Ancient ceramic glazes can be divided into high-temperature glazes and low-temperature glazes according to the firing temperature. The formula for high-temperature glazes such as copper red glaze does not contain lead oxide, while the formula for low-temperature glazes such as gold ruby-pink enamel usually contains lead oxide. Generally speaking, the main components of ancient ceramic glazes include silicon dioxide, aluminum oxide, calcium oxide, as well as certain amounts of sodium oxide, potassium oxide, magnesium oxide, iron oxide, etc.

Literature data show that the refractive indices of silica and alumina at 587.6 nm (Helium yellow line) are 1.46 [19] and 1.77 [20], respectively (see also <https://refractiveindex.info>) There are no authoritative data for the refractive indices of lead oxide and calcium oxide, but we know that in the production of modern optical glass, lead oxide is often used to increase the refractive index of products. For example, the refractive index of dense flint glass H-ZF73 can reach 1.96 at 587.6 nm [21]. Therefore, in our calculations, the range of glaze refractive index is set to 1.46–1.96.

3 Results and discussion

3.1 Copper red glaze

In our previous work, we have calculated the corresponding reflection spectra of simulated copper red glaze with copper particle diameters of 20 nm, 50 nm, 100 nm, and 200 nm under different volume fractions. In order to keep consistency with previous work, the other parameters are set as follows:

The diameter of copper nanoparticles d is a common parameter in this work and is set to be 50 nm based on previous experimental results;

Volume fraction of copper nanoparticles ω is always a variable to be studied, with values of 3×10^{-5} , 1×10^{-4} , 3×10^{-4} , 1×10^{-3} , 3×10^{-3} , 1×10^{-2} and 3×10^{-2} , respectively;

When used as a variable to be studied, the values of refractive index n are 1.46, 1.56, 1.66, 1.76, 1.86, and 1.96; as an ordinary parameter, the refractive index of copper red glaze is set as 1.52;

When used as a variable to be studied, the thicknesses of glaze T are 50 μm , 100 μm , 300 μm and 400 μm ; as an ordinary parameter, the thickness of glaze is set as 200 μm ;

Glaze transparency: In this work, the transparency of glaze is set to be 0.9/200 μm , which means that the intensity of transmitted light will decrease by 10% for every 200 μm .

3.1.1 Refractive index and copper red glaze

Figure 2 shows the calculated reflection spectra of the copper red glaze with refractive indices of 1.46, 1.56, 1.66, 1.76, 1.86 and 1.96 for the glaze layer. It can be seen that when the volume fraction of copper nanoparticles is very low, with the increase of refractive index, the reflectivity of the system to short-wavelength light increases, while the reflectivity of long-wavelength light decreases, resulting in a low reflectivity valley at around 600 nm. When the volume fraction of copper nanoparticles is high, the reflectivity of the system gradually increases with the increase of the refractive index, and a broad peak of reflectivity is formed around 620 nm.

In order to intuitively understand the effect of the refractive index change on the color, we calculated the corresponding L*a*b* values based on the reflection spectrum calculated in Fig. 1 and simulated the corresponding color, as shown in Table 1.

As can be seen from Table 1, when the volume fraction is less than 1%, the a* and b* values decrease as the refractive index increases. If $a^* > 15$ is taken as the criterion for red, then the refractive index should be below 1.56, and the most suitable volume fraction should be around 1×10^{-4} .

3.1.2 Thickness and copper red glaze

Figure 3 shows the calculated reflection spectrum of copper red glaze with thickness of 50 μm , 100 μm , 300 μm and 400 μm , respectively. It should be noted that the thickness discussed here is the thickness of the red layer in the copper red glaze, rather than the total thickness of the glaze. It can be seen that with the increase of thickness, the reflectivity of the system for all wavelengths decreases, especially for long-wavelength light, which is consistent with our intuition.

Table 2 gives the L*a*b* values for each reflection spectrum in Fig. 3 and simulates the corresponding colors. It is not difficult to see that for a given thickness, the chromaticity value a* and b* both increase first and then decrease with the increase of volume fraction, while as the thickness increases, the volume fraction required to reach the maximum of a* and b* becomes smaller and smaller.

3.2 Gold ruby-pink enamel

According to previous literature, the diameter of gold nanoparticles selected in this work ranged from 10 to 120 nm, and the volume fraction ranged from 3×10^{-6} to 3×10^{-3} . Considering that the refractive index of gold ruby-pink enamel generally contains lead oxide, the refractive index will be higher than that of traditional high-temperature calcium glaze, we first take the refractive index $n = 1.7$ to calculate and find the appropriate particle size and volume fraction, and then study the effect of refractive index on the optical effect of gold ruby-pink enamel.

When the glaze thickness T is used as the variable to be studied, the values are 50 μm , 100 μm , 300 μm and 400 μm ; when used as a common parameter, it is set to be 200 μm . The values of the body-glaze interface reflectivity r_2 are 0.8, 0.7, 0.6, 0.5 and 0.4 when used as the variable to be studied, and 0.7 when used as a common parameter.

3.2.1 Diameter and gold ruby-pink enamel

Figure 4 shows the reflection spectra of gold ruby-pink enamel with different particle diameters, and their characteristics, especially those with small particle sizes, are very close to previously reported reflection spectra: The reflectivity is high at 650–800 nm, medium at 300–500 nm, and there is a trough of reflectivity at around 570 nm. With the increase of the volume fraction of gold

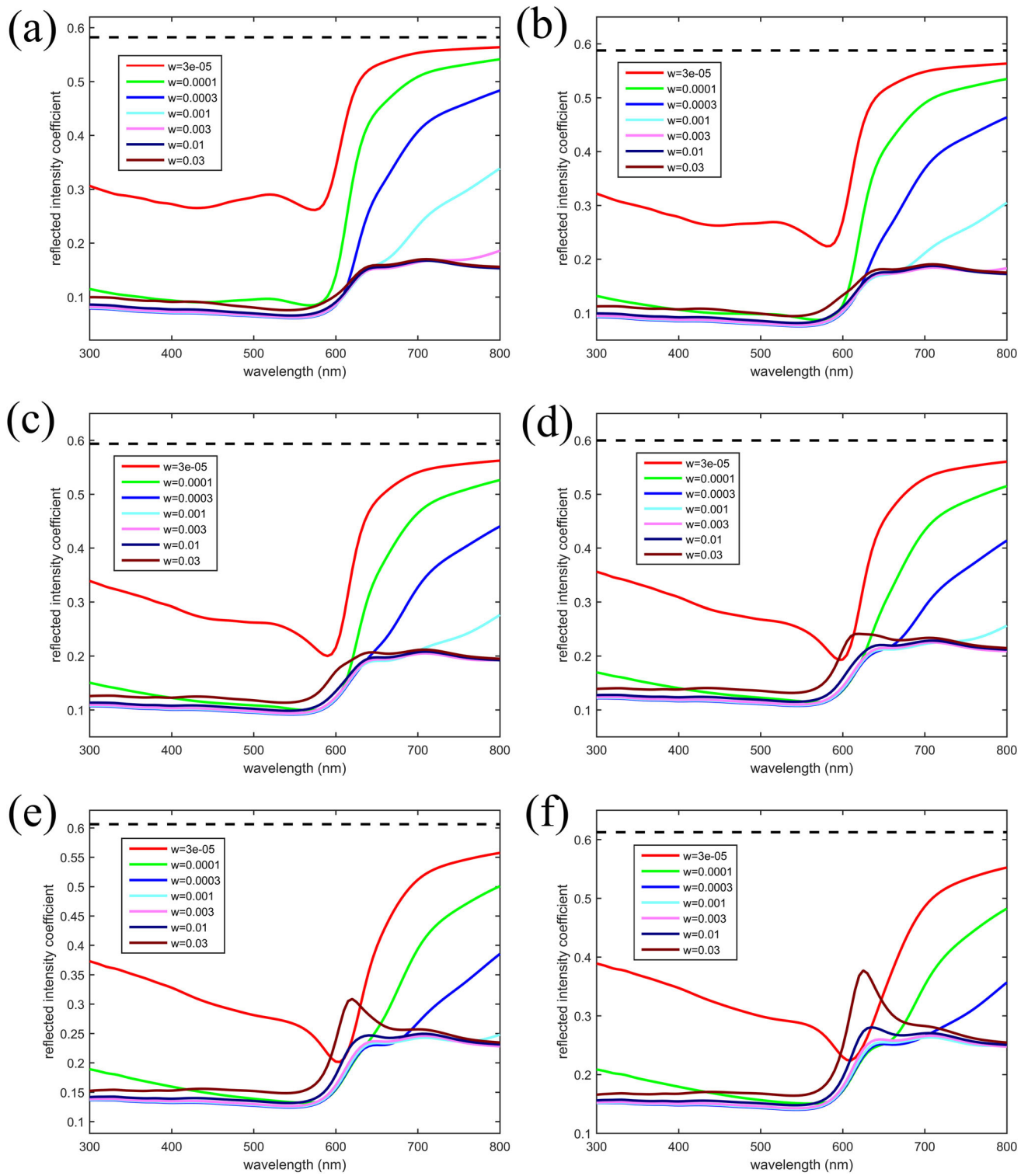


Fig. 2 Reflection spectra of copper red glaze with different refractive index. The nanoparticles dispersed in the glaze are metallic copper particles, the diameter is 50 nm, and the thickness of glaze is set as 200 μm . The black dotted lines represent the reflection spectra of pure transparent glaze without any second-phase particles. **a-f** corresponds to the cases where the refractive indices of the transparent glaze are 1.46, 1.56, 1.66, 1.76, 1.86, and 1.96, respectively

nano-particles, the reflectivity of 300–500 nm gradually decreases to a level similar to that of the trough, which intuitively seems to be that the trough is gradually smoothed out.

From the results in Table 3, we can see that if the chromaticity value $a^* > 15$ continues to be used as the criterion for exhibiting red, then it is only possible to obtain a pink hue when the particle diameter of the gold nanoparticles is in the range of 10–40 nm and

Table 1 L*a*b* values of copper red glaze with different refractive index. The nanoparticles dispersed in the glaze are metallic copper particles, the diameter is 50 nm, and the thickness of glaze is set as 200 μm

Volume fraction		3×10^{-5}	1×10^{-4}	3×10^{-4}	1×10^{-3}	3×10^{-3}	1×10^{-2}	3×10^{-2}
1.46 [†]	L*	62.0	41.5	33.7	32.5	32.7	33.4	35.6
	a*	10.8	24.4	18.5	11.5	11.1	10.9	10.2
	b*	5.1	9.0	4.1	1.6	1.4	1.1	0.2
	Color**							
1.52	L*	60.2	40.3	34.6	33.9	34.2	35.0	37.6
	a*	10.7	22.1	15.4	11.0	11.0	10.8	10.2
	b*	3.0	6.2	3.0	1.6	1.5	1.4	0.8
	Color							
1.56	L*	59.4	40.4	36.0	35.7	36.0	36.9	39.5
	a*	10.1	19.6	13.4	10.5	10.5	10.4	10.0
	b*	1.5	4.5	2.5	1.6	1.6	1.5	1.2
	Color							
1.66	L*	57.8	41.1	38.7	38.7	39.0	40.1	43.1
	a*	7.3	14.4	10.8	9.9	10.1	10.2	10.7
	b*	-2.1	1.7	1.9	1.7	1.7	1.9	2.5
	Color							
1.76	L*	57.4	42.8	41.4	41.5	41.9	43.0	46.3
	a*	3.6	10.7	9.6	9.6	9.8	10.4	12.2
	b*	-4.6	0.2	1.8	1.8	1.9	2.3	3.8
	Color							
1.86	L*	58.3	45.0	43.9	44.1	44.4	45.6	49.0
	a*	0.2	8.7	9.2	9.3	9.6	10.7	14.0
	b*	-5.8	-0.4	1.8	1.9	2.0	2.7	4.8
	Color							
1.96	L*	59.9	47.4	46.3	46.4	46.8	47.9	51.3
	a*	-1.6	7.7	8.9	9.0	9.4	10.9	15.3
	b*	-5.9	-0.7	1.9	1.9	2.1	2.9	5.3
	Color							

[†]: the first column refers to the refractive index of the glaze; **: the colors are recreated by <https://www.qtccolor.com/secaiku/tool/convert?m=lab>

the volume fraction is below 3×10^{-5} . As the volume fraction increases, the value b* turns from negative to positive, and the red color becomes darker. As the particle diameter increases, the glaze will appear grayish-white at lower volume fractions. However, at higher volume fractions, the glaze will appear brownish-yellow: Although the chromaticity value a* also exceeds 15, the value b* representing the yellow-blue hue is close to or even larger.

Based on the above results, we speculate that in order to obtain the typical pink color of ancient gold ruby-pink enamel, the diameter of the gold particles should be around 20 nm.

3.2.2 Refractive index and gold ruby-pink enamel

Next, we will study the influence of the glaze refractive index on the color of the gold ruby-pink enamel. As in our previous calculation for copper red glaze, we set the refractive index range to be 1.46–1.96 and the particle diameter of gold nanoparticles to be 20 nm.

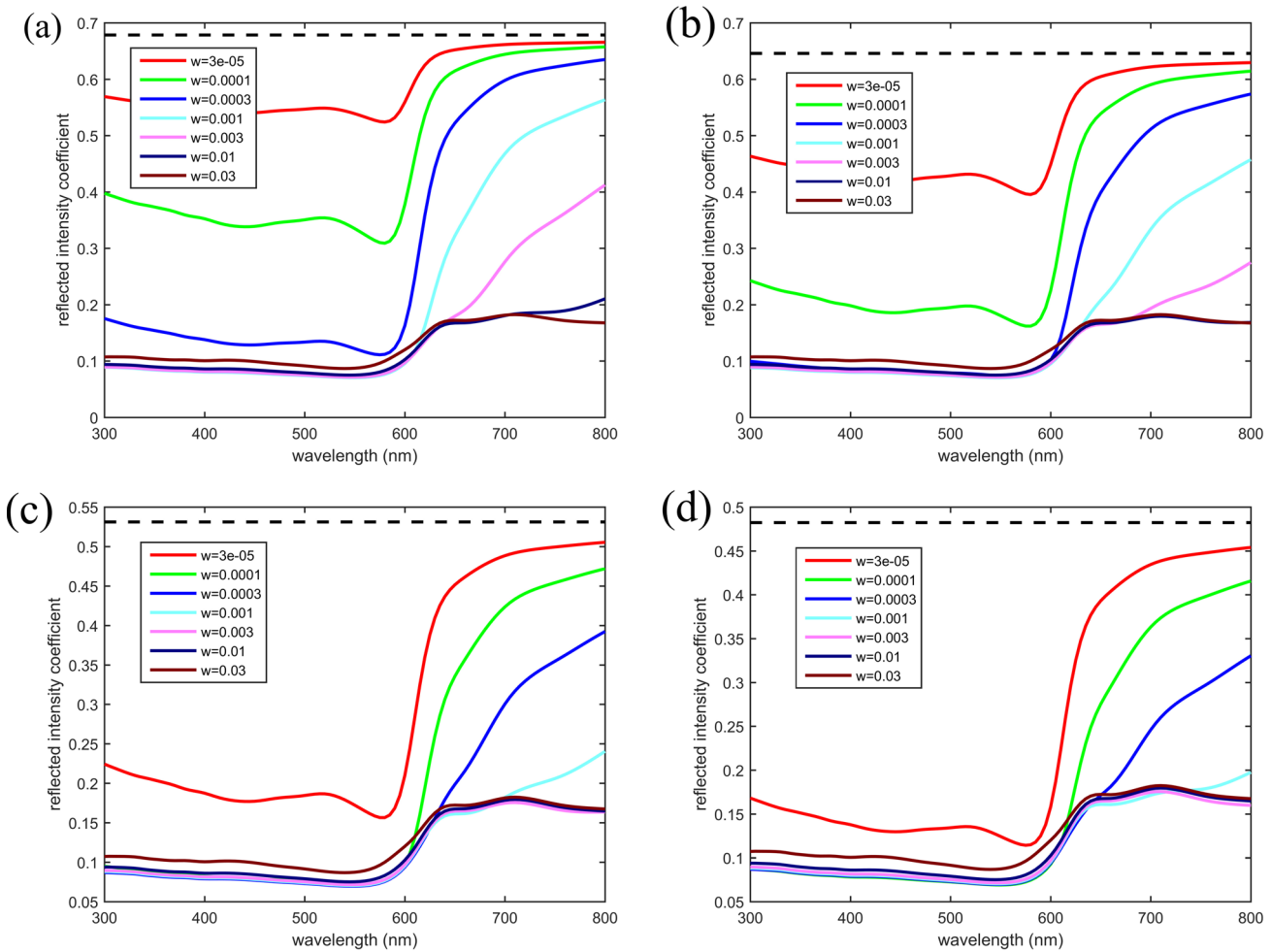


Fig. 3 Reflection spectra of copper red glaze with different thickness. The nanoparticles dispersed in the glaze are metallic copper particles, the diameter here is 50 nm, and the refractive index is 1.52. The black dotted lines represent the reflection spectra of pure transparent glaze without any second-phase particles. **a-d** corresponds to the cases where the thickness of the transparent glaze are 50 μm , 100 μm , 300 μm and 400 μm , respectively

Figure 5 shows the calculated reflection spectra of the gold ruby-pink enamel when the refractive indices of the glaze layer are 1.46, 1.56, 1.66, 1.76, 1.86 and 1.96, respectively. As the refractive index increases, the shapes of the reflection spectra do not appear to change much, but the position of the reflectivity trough gradually shifts to longer wavelengths, and the width of this trough also increases.

The position of the reflectivity trough seems to have shifted just a few tens of nanometers, but in reality, its impact is really significant, which is particularly evident in Table 4. When the refractive index changes from 1.46 to 1.96, the chromaticity value a^* can be reduced from about 40 to 5, which is reflected in the color that both pink and dark red disappear, leaving only blue-gray. Therefore, in order to obtain a high-quality gold ruby-pink enamel, the refractive index of the glaze should not be too high, in other words, there should not be too much lead oxide in the glaze recipe.

3.2.3 Thickness and gold ruby-pink enamel

Figure 6 shows the calculated reflection spectra of the gold ruby-pink enamel with thickness 50 μm , 100 μm , 300 μm and 400 μm . It is not difficult to see that with the increase of thickness, the reflectivity of the system to all wavelengths decreases.

From the results in Table 5, the glaze color gradually darkens as the thickness increases. For a given thickness, the chromaticity values a^* and b^* both increase first and then decrease with the increase of volume fraction. As the thickness increases, the volume fraction required to reach the maximum value of a^* and b^* becomes smaller and smaller. Both of these points are consistent with the copper red glaze. However, under this series of thickness conditions, the gold ruby-pink enamel can exhibit an a^* value exceeding 25, and the required volume fraction is less than that of copper red glaze, which indicates that the coloring ability of gold is stronger than that of copper.

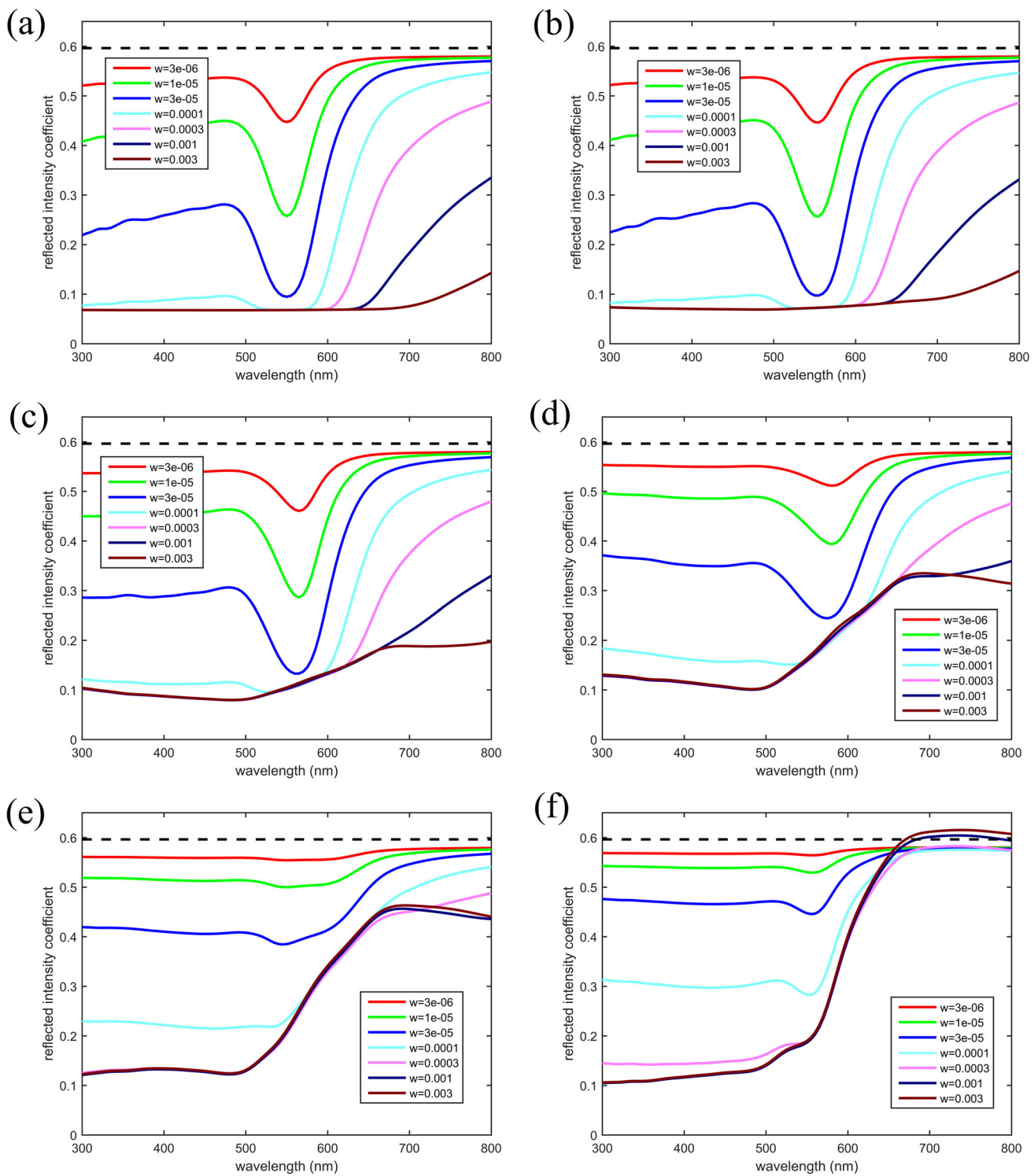


Fig. 4 Reflection spectra of gold ruby-pink enamel with different diameters. The nanoparticles dispersed in the glaze are metallic gold particles, the refractive index here is 1.7, and the thickness of the glaze is 200 μm . The black dotted lines represent the reflection spectra of pure transparent glaze without any second-phase particles. **a-f** corresponds to the cases where the diameters of gold nanoparticles are 10 nm, 20 nm, 40 nm, 60 nm, 80 nm and 120 nm, respectively

3.2.4 Body reflectivity and gold ruby-pink enamel

Finally, we will discuss the relationship between the reflectivity of the body and the color of the gold ruby-pink enamel.

Table 2 L*a*b* values of copper red glaze with different thickness. The nanoparticles dispersed in the glaze are metallic copper particles with diameter 50 nm, the refractive index is 1.52

Volume fraction		3×10^{-5}	1×10^{-4}	3×10^{-4}	1×10^{-3}	3×10^{-3}	1×10^{-2}	3×10^{-2}
50 μm^{\dagger}	L*	79.1	66.7	46.6	35.9	34.8	35.5	38.0
	a*	3.1	9.7	21.9	18.1	11.4	10.6	10.0
	b*	0.8	2.7	6.5	4.0	1.7	1.3	0.7
	Color**							
100 μm	L*	71.9	53.4	37.7	34.7	34.7	35.5	38.0
	a*	5.9	16.8	22.2	12.6	10.8	10.6	10.0
	b*	1.6	4.9	5.9	2.1	1.5	1.3	0.7
	Color							
200 μm	L*	60.2	40.3	34.6	33.9	34.2	35.0	37.6
	a*	10.7	22.1	15.4	11.0	11.0	10.8	10.2
	b*	3.0	6.2	3.0	1.6	1.5	1.4	0.8
	Color							
300 μm	L*	51.7	36.6	34.5	34.4	34.7	35.5	38.0
	a*	14.1	19.5	12.1	10.6	10.7	10.6	10.0
	b*	4.0	4.8	2.0	1.5	1.5	1.3	0.7
	Color							
400 μm	L*	45.6	35.2	34.3	34.4	34.7	35.5	38.0
	a*	16.1	16.4	10.9	10.6	10.7	10.6	10.0
	b*	4.5	3.5	1.6	1.5	1.5	1.3	0.7
	Color							

[†]: the first column refers to the thickness of the transparent glaze; **: the colors are recreated by <https://www.qtccolor.com/secaiku/tool/convert?m=lab>

Figure 7 shows the calculated reflection spectra of the gold ruby-pink enamel with different body reflectivity. It seems that the body reflectivity almost has no effect on the shapes and peak positions of the reflection spectra, and the main effect is the stretching and compression of the ordinate.

The above qualitative analysis is even more evident in Table 6: Although the color blocks in each column corresponding to different body reflectivity have different shades, they intuitively appear to belong to the same category of colors, while the color blocks in each row do not seem to belong to the same category. According to the quantitative data, the absolute values of L*, a* and b* all decrease with the decrease of body reflectivity, but the ratio of a* to b* remains basically unchanged. In fact, in another commonly used L*c*h* color space, $h^* = \arctan(b^*/a^*)$ represents the hue of the color, therefore when the ratio of a* to b* remains constant, the hue of the color also remains unchanged, and it naturally appears to belong to the same color category.

3.3 A brief discussion

We have analyzed the colors produced by copper nanoparticles and gold nanoparticles under different conditions such as refractive index, glaze thickness, particle volume fraction, etc., and the results show that there are significant differences between these two systems. In order to gain a deeper understanding of this behavior, we need to know the scattering and absorption capabilities of these two kinds of nanoparticles for light [22], as shown in Fig. 8.

The scattering coefficient Q_{sca} , forward/backward scattering ratio r_{fb} , and absorption coefficient Q_{abs} of copper and gold nanoparticles for light of different wavelengths are shown in Fig. 7, and the location and intensity of the scattering and absorption peaks of them are given in Table 7. From these results, we can make the following findings:

- For both copper and gold nanoparticles, when the particle diameter is less than 40 nm, the scattering coefficient is much smaller than the absorption coefficient; when the particle size is about 60 nm, the scattering coefficient and absorption coefficient are basically the same; for larger particle diameters, the scattering coefficient is slightly higher than the absorption coefficient. Therefore, when the diameter of the second-phase particle is very small, it is the absorption of light that dominates.

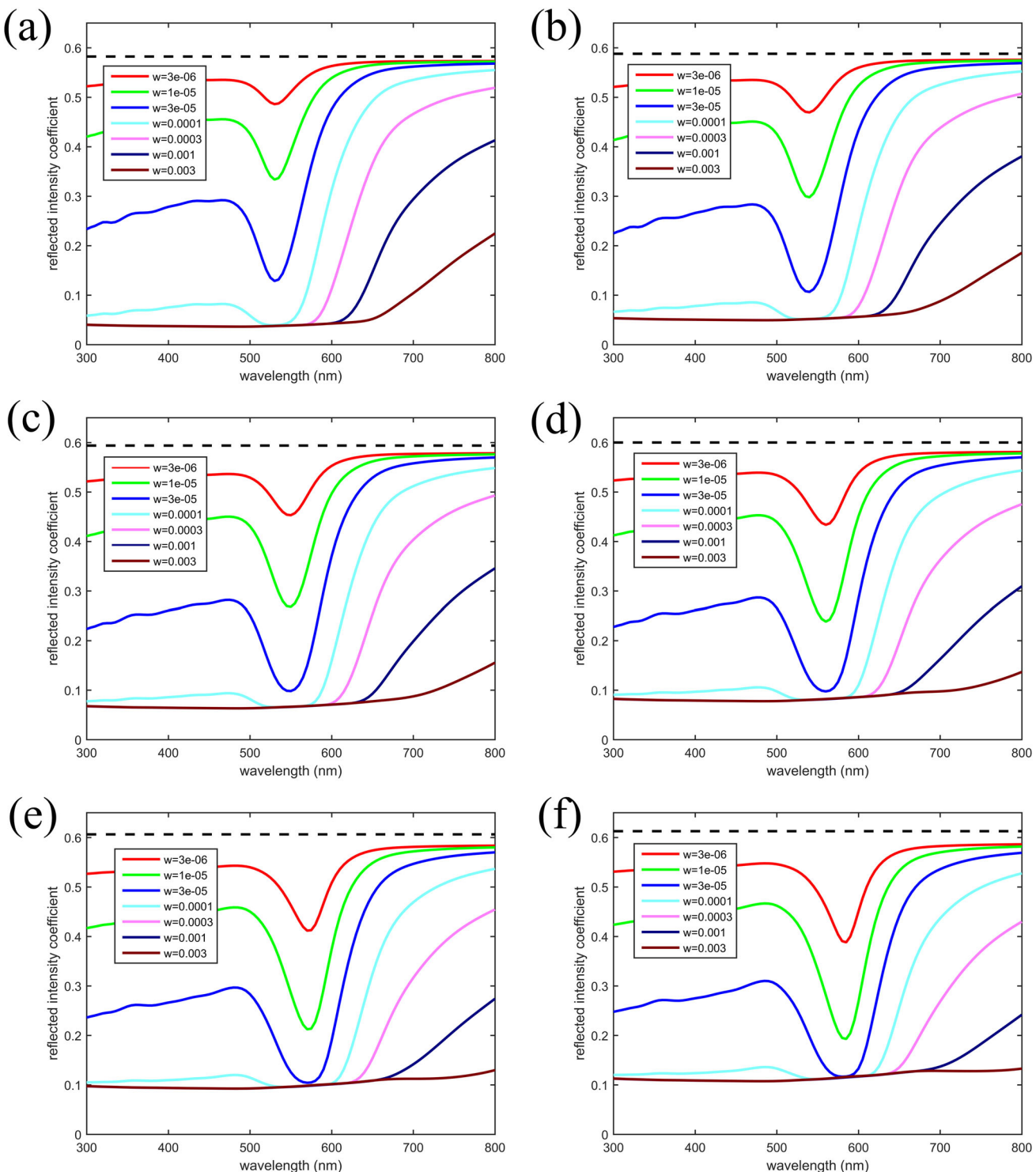


Fig. 5 Reflection spectra of gold ruby-pink enamel with different refractive index. The nanoparticles dispersed in the glaze are metallic gold particles, the diameter here is 20 nm, and the thickness of the glaze is 200 μm . The black dotted lines represent the reflection spectra of pure transparent glaze without any second-phase particles. **a-f** corresponds to the cases where the refractive indices of the transparent glaze are 1.46, 1.56, 1.66, 1.76, 1.86, and 1.96, respectively

- 2) For gold nanoparticles, with the increase of particle size, the peak position of the absorption coefficient of gold nanoparticles shifted from 550 to 595 nm and then back to 555 nm; the peak position of the scattering coefficient shifted from 555 to 695 nm and back to 655 nm. However, the peak shape of the absorption coefficient of copper nanoparticles is not obvious. With the increase of particle diameter, the peak position of the absorption coefficient of copper nanoparticles shifted from 570 to 590 nm

Table 3 L*a*b* values of gold ruby-pink enamel with different diameters. The nanoparticles dispersed in the glaze are metallic gold particles, the refractive index here is 1.7, and the thickness of glaze is set as 200 μm

Volume fraction		3×10^{-6}	1×10^{-5}	3×10^{-5}	1×10^{-4}	3×10^{-4}	1×10^{-3}	3×10^{-3}
10 nm [†]	L*	76.4	68.0	53.6	38.8	33.1	31.5	31.3
	a*	5.4	15.4	29.8	28.1	10.6	1.2	0.3
	b*	-3.0	-7.5	-9.5	4.0	3.2	0.4	0.2
	Color							
20 nm	L*	76.3	67.9	53.4	38.9	33.8	32.5	32.5
	a*	5.1	14.4	28.0	26.1	10.0	2.4	1.8
	b*	-3.2	-8.0	-10.2	3.5	3.7	1.5	1.4
	Color**							
40 nm	L*	76.7	68.9	55.2	42.2	39.3	39.1	39.4
	a*	2.8	8.3	17.6	18.5	10.7	8.6	8.6
	b*	-3.0	-7.8	-10.7	3.6	8.5	8.1	8.5
	Color							
60 nm	L*	78.1	72.8	62.1	50.0	47.9	48.2	48.7
	a*	0.3	1.3	5.0	13.4	14.5	14.5	14.6
	b*	-1.5	-4.2	-6.4	5.9	15.7	16.1	16.6
	Color							
80 nm	L*	79.4	76.5	69.8	58.2	54.6	54.9	55.3
	a*	0.3	1.0	3.4	12.6	18.3	18.6	18.6
	b*	-0.2	-0.6	-0.3	8.0	20.7	21.6	21.9
	Color							
120 nm	L*	80.1	78.6	74.8	65.2	56.7	56.2	56.6
	a*	0.6	1.8	5.1	14.0	23.4	25.1	25.2
	b*	0.1	0.4	1.4	6.2	19.4	24.5	24.7
	Color							

[†]: the first column refers to the diameters of metallic gold nanoparticles; **: the colors are recreated by <https://www.qtccolor.com/secaiku/tool/convert?m=lab>

and back to 560 nm, and the peak position of the scattering coefficient shifted from 590 to 640 nm and back to 625 nm. Overall,

the shift amplitude of the peak position of gold particles changing with particle size is much larger than that of copper particles. At the same particle diameter, the absorption coefficient and scattered absorption peaks of gold nanoparticles are higher than those of copper nanoparticles. This explains why gold nanoparticles have a stronger coloring ability than copper nanoparticles.

- 3) In the short-wave region to the left of the absorption/scattering coefficient peaks, the scattering coefficients and absorption coefficients of gold nanoparticles are slightly lower than those of copper nanoparticles. Therefore, in the reflection spectra of copper red glaze, the reflection of the short-wave region below 600 nm is relatively low; while in the reflection spectra of gold ruby-pink enamel, the short-wave region still has a certain reflectivity, so there is some blue component in the reflected light and shows a pink hue.

In addition, we need to point out a fact. Some scholars have argued that the coloration mechanism of such metal nanoparticles by Mie scattering theory is too out of fashion and should be replaced by more advanced local surface plasmon resonance (LSPR) [23, 24]. In fact, according to Born's *Principles of Optics*, the surface plasmon oscillation behavior can actually be determined by the dielectric function of metal particles [25], which means that it is actually a derived result of Mie scattering theory. Our calculation results on the reflectance spectra of copper and gold nanoparticles have well demonstrated this point.

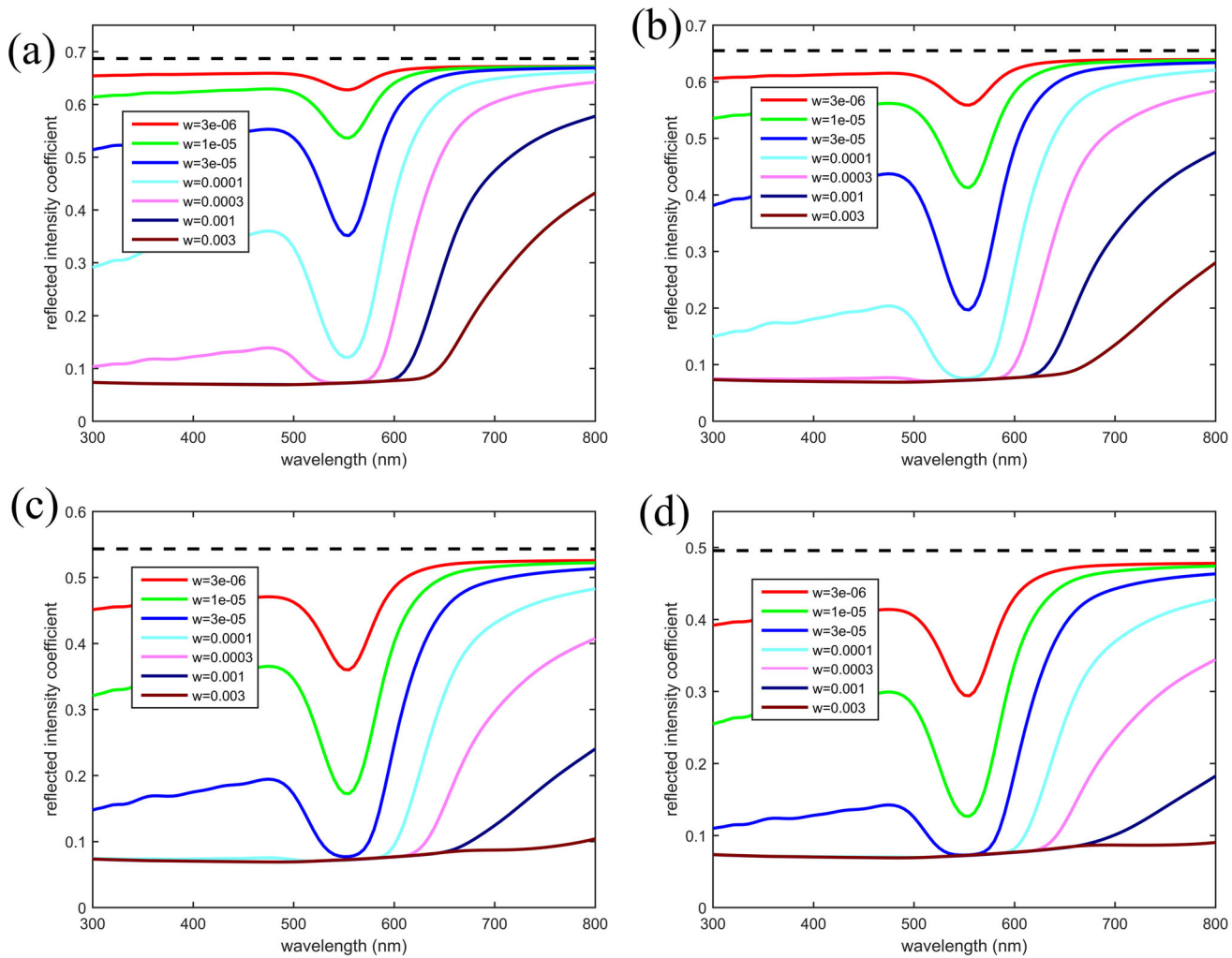


Fig. 6 Reflection spectra of gold ruby-pink enamel with different thickness. The nanoparticles dispersed in the glaze are metallic copper particles, the diameter here is 20 nm, and the refractive index is 1.7. The black dotted lines represent the reflection spectra of pure transparent glaze without any second-phase particles. **a-d** corresponds to the cases where the thickness of the transparent glaze are 50 μm , 100 μm , 300 μm and 400 μm , respectively

Table 4 L*a*b* values of gold ruby-pink enamel with different refractive indices. The nanoparticles dispersed in the glaze are metallic gold particles with diameter 20 nm, and the thickness of glaze is set as 200 μm

Volume fraction		3×10^{-6}	1×10^{-5}	3×10^{-5}	1×10^{-4}	3×10^{-4}	1×10^{-3}	3×10^{-3}
1.46 [†]	L*	77.8	72.4	60.9	43.5	31.6	24.8	23.6
	a*	4.5	13.3	30.2	43.8	32.6	10.1	2.7
	b*	-0.5	-1.1	0.9	16.6	15.6	4.0	1.8
	Color**							
1.56	L*	77.2	70.4	57.3	40.6	31.7	28.0	27.6
	a*	5.2	15.2	32.2	38.7	21.8	5.1	2.1
	b*	-1.5	-3.8	-3.9	10.5	8.6	2.3	1.6
	Color							
1.66	L*	76.6	68.6	54.3	39.1	33.0	31.3	31.2
	a*	5.3	15.2	30.1	30.1	12.7	2.9	1.9
	b*	-2.7	-6.8	-8.5	5.2	4.7	1.7	1.5
	Color							
1.70	L*	76.3	67.9	53.4	38.9	33.8	32.5	32.5
	a*	5.1	14.4	28.0	26.1	10.0	2.4	1.8
	b*	-3.2	-8.0	-10.2	3.5	3.7	1.5	1.4
	Color							
1.76	L*	76.0	67.1	52.4	39.0	35.1	34.4	34.4
	a*	4.4	12.3	23.4	20.1	6.8	2.0	1.7
	b*	-3.9	-9.6	-12.2	1.5	2.7	1.4	1.4
	Color							
1.86	L*	75.6	66.2	51.9	40.0	37.6	37.3	37.3
	a*	2.1	6.3	13.1	11.3	3.7	1.7	1.7
	b*	-4.8	-11.6	-14.2	-0.7	1.8	1.3	1.4
	Color							
1.96	L*	75.6	66.2	52.7	41.7	40.0	40.0	40.0
	a*	-1.2	-1.8	1.9	5.1	2.3	1.6	1.7
	b*	-5.4	-12.3	-14.4	-1.7	1.4	1.3	1.4
	Color							

[†]: the first column refers to the refractive index of the glaze; **: the colors are recreated by <https://www.qtccolor.com/secaiku/tool/convert?m=lab>

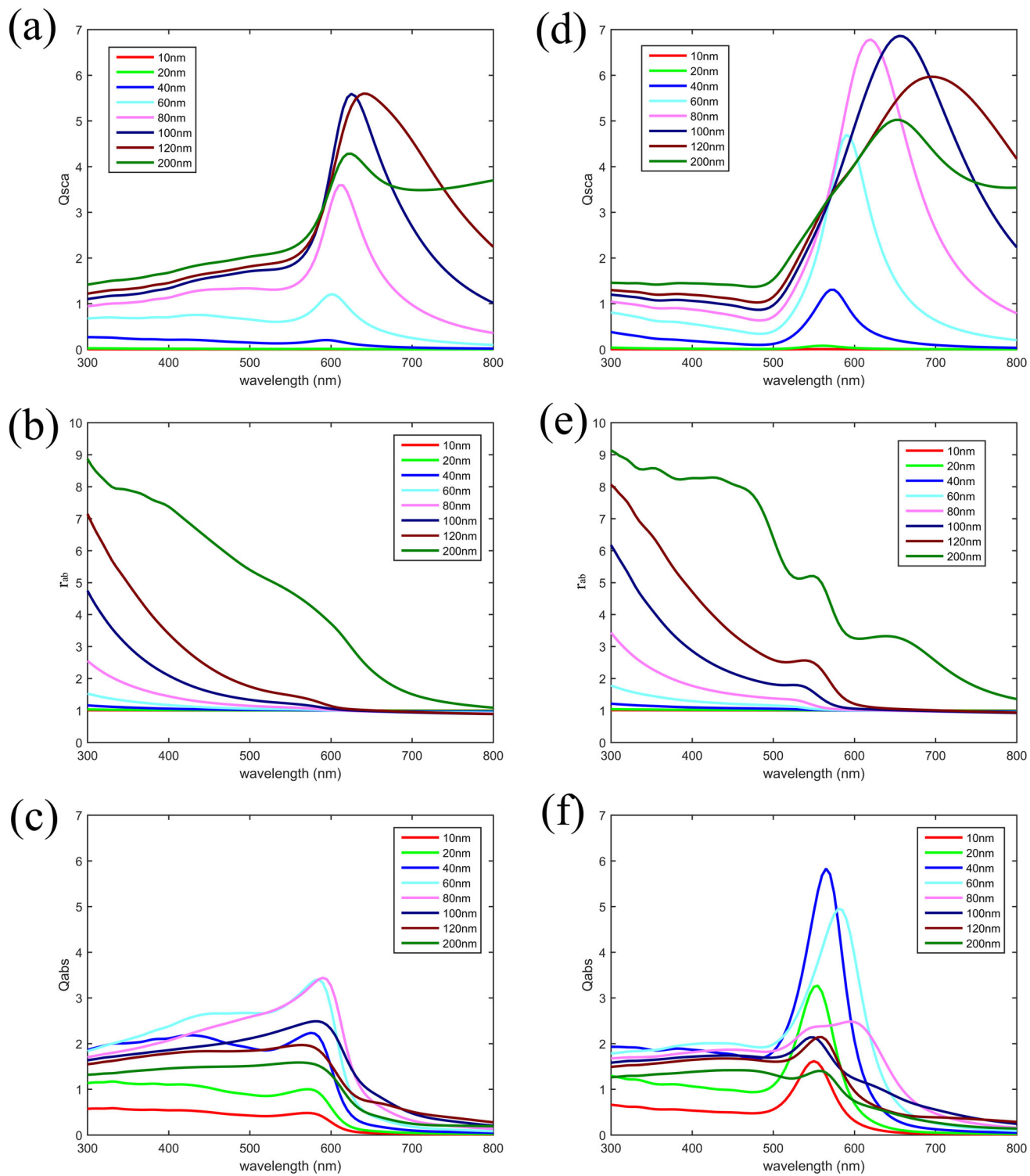


Fig. 7 Reflection spectra of gold ruby-pink enamel with different body reflectivity. The nanoparticles dispersed in the glaze are metallic gold particles, the diameter here is 20 nm, the refractive index is 1.7 and the thickness is 200 μm . The black dotted lines represent the reflection spectra of pure transparent glaze without any second-phase particles. **a-d** corresponds to the cases where the body reflectivity are 0.8, 0.6, 0.5 and 0.4, respectively

Table 5 L*a*b* values of gold ruby-pink enamel with different thickness. The nanoparticles dispersed in the glaze are metallic gold particles with diameter 20 nm, and the refractive index is 1.7

Volume fraction		3×10^{-6}	1×10^{-5}	3×10^{-5}	1×10^{-4}	3×10^{-4}	1×10^{-3}	3×10^{-3}
50 μm^{\dagger}	L*	84.4	81.6	74.7	59.0	42.9	34.6	32.7
	a*	1.5	4.6	12.3	28.2	32.5	14.0	3.5
	b*	-1.0	-2.9	-7.2	-11.5	-0.3	5.0	1.8
	Color**							
100 μm	L*	81.5	76.5	65.5	47.5	36.7	33.0	32.5
	a*	2.8	8.5	20.4	32.9	21.7	5.6	2.0
	b*	-1.8	-5.1	-10.3	-6.4	6.2	2.4	1.5
	Color							
200 μm	L*	76.3	67.9	53.4	38.9	33.8	32.5	32.5
	a*	5.1	14.4	28.0	26.1	10.0	2.4	1.8
	b*	-3.2	-8.0	-10.2	3.5	3.7	1.5	1.4
	Color							
300 μm	L*	71.6	61.0	46.3	35.9	33.0	32.5	32.5
	a*	7.0	18.4	28.8	18.4	5.5	1.9	1.8
	b*	-4.3	-9.3	-6.7	5.3	2.4	1.4	1.4
	Color							
400 μm	L*	67.3	55.5	42.0	34.5	32.7	32.5	32.5
	a*	8.5	20.7	26.7	13.0	3.6	1.8	1.8
	b*	-5.1	-9.5	-2.9	4.5	1.8	1.4	1.4
	Color							

[†]: the first column refers to the thickness of the glaze; **: the colors are recreated by <https://www.qtccolor.com/secaiku/tool/convert?m=lab>

Table 6 L*a*b* values of gold ruby-pink enamel with different body reflectivity. The nanoparticles dispersed in the glaze are metallic gold particles, the diameter here is 20 nm, the refractive index is 1.7, and the thickness is 200 μm

Volume fraction		3×10^{-6}	1×10^{-5}	3×10^{-5}	1×10^{-4}	3×10^{-4}	1×10^{-3}	3×10^{-3}
0.8 [†]	L*	80.1	71.1	55.6	39.7	34.0	32.6	32.5
	a*	5.4	15.4	30.1	28.7	11.1	2.5	1.8
	b*	-3.4	-8.5	-11.0	3.8	4.1	1.6	1.4
	a*/b*	-1.6	-1.8	-2.7	7.5	2.7	1.6	1.3
	Color**							
0.7	L*	76.3	67.9	53.4	38.9	33.8	32.5	32.5
	a*	5.1	14.4	28.0	26.1	10.0	2.4	1.8
	b*	-3.2	-8.0	-10.2	3.5	3.7	1.5	1.4
	a*/b*	-1.6	-1.8	-2.7	7.4	2.7	1.6	1.3
	Color							
0.6	L*	72.2	64.4	51.1	38.0	33.6	32.5	32.5
	a*	4.7	13.4	25.7	23.3	8.8	2.3	1.8
	b*	-3.0	-7.4	-9.3	3.2	3.4	1.5	1.4
	a*/b*	-1.6	-1.8	-2.8	7.3	2.6	1.5	1.3
	Color							
0.5	L*	67.8	60.6	48.6	37.1	33.4	32.5	32.5
	a*	4.3	12.2	23.1	20.3	7.7	2.2	1.8
	b*	-2.7	-6.8	-8.4	2.9	3.0	1.5	1.4
	a*/b*	-1.6	-1.8	-2.8	7.0	2.5	1.5	1.3
	Color							
0.4	L*	62.8	56.5	45.9	36.2	33.2	32.5	32.5
	a*	3.9	10.8	20.2	17.1	6.5	2.1	1.8
	b*	-2.4	-6.0	-7.2	2.6	2.7	1.5	1.4
	a*/b*	-1.6	-1.8	-2.8	6.7	2.4	1.5	1.3
	Color							

[†]: the first column refers to the body reflectivity; **: The colors are recreated by <https://www.qtccolor.com/secaiku/tool/convert?m=lab>

Table 7 The positions and intensities of scattering and absorption peaks of copper and gold nanoparticles with different diameters

Diameter		10 nm	20 nm	40 nm	60 nm	80 nm	100 nm	120 nm	200 nm
Copper red glaze	SPP	590	590	595	600	610	625	640	625
	SPI	0.0006	0.011	0.20	1.21	3.59	5.59	5.60	4.28
	APP	570	570	575	585	590	580	565	560
	API	0.48	1.00	2.23	3.40	3.44	2.49	1.97	1.59
Gold ruby-pink enamel	SPP	555	560	575	590	620	655	695	655
	SPI	0.005	0.078	1.30	4.69	6.78	6.86	5.97	5.02
	APP	550	555	565	580	595	545	560	555
	API	1.62	3.27	5.83	4.95	2.48	2.14	2.14	1.40

SPP: Scattering peak position; SPI: Scattering peak intensity; APP: Absorption peak position; API: Absorption peak intensity

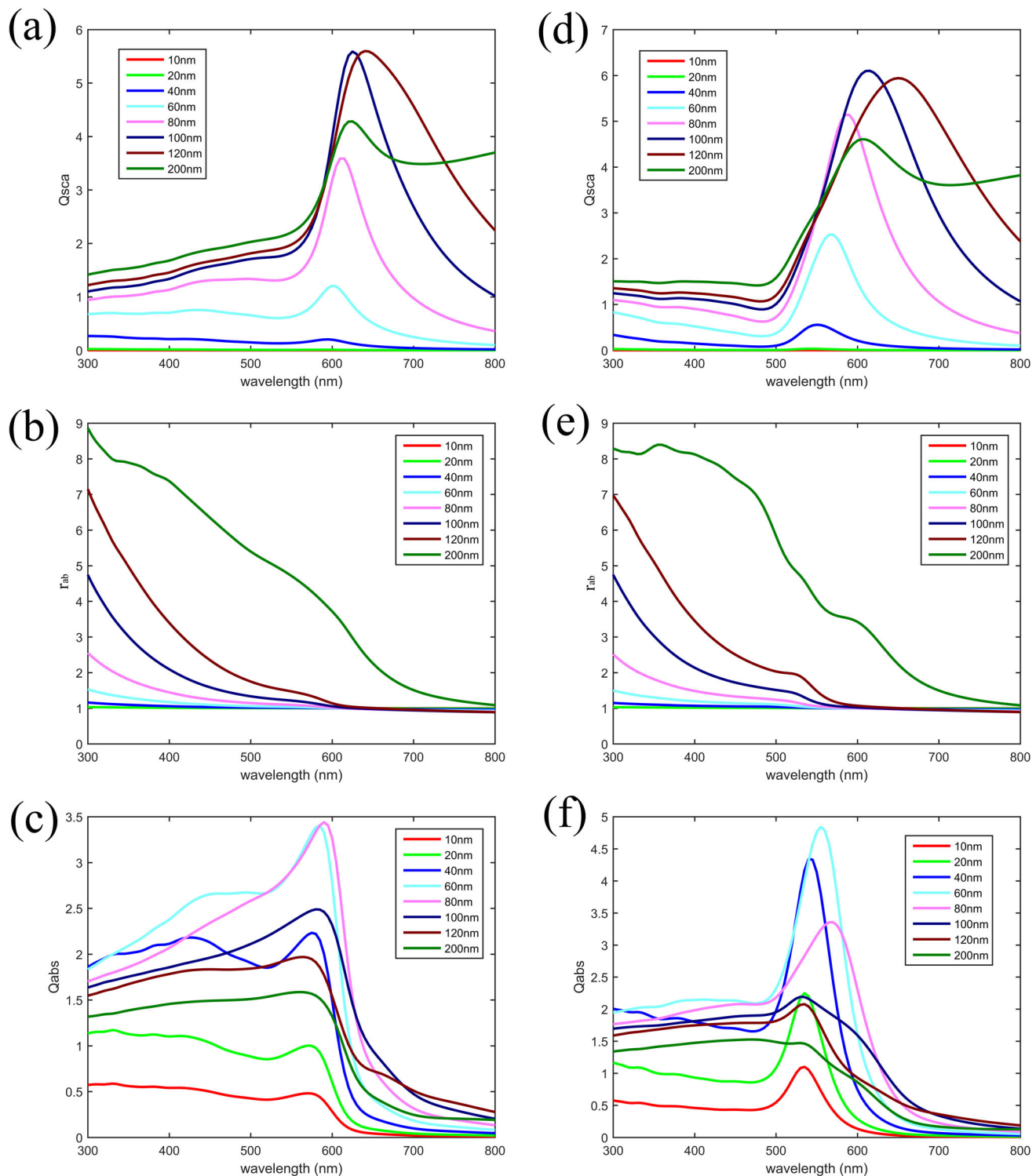


Fig. 8 Scattering coefficient Q_{sca} , forward/backward scattering ratio r_{fb} and absorption coefficient Q_{abs} of metal particles with different diameters for light of different wavelengths. **a-c** copper nanoparticles, with the refractive index of transparent glaze 1.52; **d-f** gold nanoparticles, with the refractive index of transparent glaze 1.7

4 Conclusion

Based on the multiple scattering theory, this article calculates the reflection spectra of copper red glaze and gold ruby-pink enamel under different conditions, and discusses the effects of parameters such as refractive index, thickness, particle diameter, and body reflectivity on glaze color. The main conclusions are as follows:

- 1) The refractive index of transparent glaze influences both copper red glaze and gold ruby-pink enamel. For copper red glaze, when the refractive index is lower, the chromaticity value a^* is higher and looks redder; for gold ruby-pink enamel, with the increase of the refractive index, the position of the reflectivity trough gradually shifts to longer wavelengths, and the color change is more drastic than that of copper red glaze.
- 2) For a given thickness, the chromaticity values a^* and b^* increase first and then decrease with the increase of the second-phase volume fraction. As the thickness increases, the volume fraction required to reach the maximum value of a^* and b^* becomes smaller and smaller.
- 3) The reflectivity of the body will affect the reflectivity of the whole system and the saturation degree of the color, but it will not change the hue.
- 4) The most suitable volume fraction of copper nanoparticles in copper red glaze is about 1×10^{-4} , while the most suitable volume fraction of gold nanoparticles in gold ruby-pink enamel is about 3×10^{-5} . In addition, the gold ruby-pink enamel can show a high a^* value with different thickness. This indicates that the coloration ability of gold is stronger than that of copper, which can be explained by the fact that the absorption coefficient and scattering coefficients peak of gold nanoparticles are higher than those of copper nanoparticles of the same particle diameter.

Acknowledgements This work was supported by National Key R&D Program of China (2023YFF0905803, 2022YFF0705503), and the National Natural Science Foundation of China (52402022). The Palace Museum Talent Program has received full support from the Hong Kong Jockey Club and exclusive donations from the Public Welfare and Charity Research Institute. We would like to express our special thanks!

Availability of data and materials The data that support the findings of this study are available from the corresponding author upon reasonable request.

References

1. J.Y. Hou, T. Pradell, J.M. Miao, The coloring function of iron oxide and phase separation in the blue glaze of Jun Ware. *Sci. Conserv. Archaeol.* **27**(02), 6–12 (2015)
2. J.Y. Hou, T. Pradell, Y. Li, J.M. Miao, Jun ware glazes: Chemistry, nanostructure and optical properties. *J. Eur. Ceram. Soc.* **38**(12), 4290–4302 (2018). <https://doi.org/10.1016/j.jeurceramsoc.2018.05.010>
3. C. Jia, G. Li, M. Guan, J. Zhao, Y. Zheng, G.Y. Wang, X.J. Wei, Y. Lei, A short but glorious porcelain glaze of early ming dynasty: new finding of raw material and colorants in the copper red glaze. *J. Eur. Ceram. Soc.* **41**(6), 3809–3815 (2021). <https://doi.org/10.1016/j.jeurceramsoc.2021.01.018>
4. G. Li, Y. Lei, The computational simulation of the reflection spectra of copper red glaze. *AIP Adv.* **12**, 095319 (2022). <https://doi.org/10.1063/5.0095570>
5. C. Noirot, L. Cormier, N. Schibille, N. Menguy, N. Trcera, E. Fonda, Comparative investigation of red and orange roman tesserae: role of Cu and Pb in colour formation. *Heritage* (2022). <https://doi.org/10.3390/heritage5030137>
6. M.Y. Yuan, J. Bonet, H. Castillo-Michel, M. Cotte, N. Schibille, B. Gratutze, T. Pradell, The role of tin and iron in the production of Spanish copper red glass from the 19th to the 20th century. *Bol. Soc. Esp. Ceram. Vidrio* **63**(2), 125–134 (2024). <https://doi.org/10.1016/j.bsecv.2023.07.005>
7. C. F. Bohren, D.R. Huffman. 1983. Absorption and Scattering of Light by Small Particles. (John Wiley & Sons, Inc., 1983), pp.83–103
8. Y.F. Xiong, W.Q. He. 2005. Pigmentation for red glazes and colours in Qing Dynasty porcelain. *Science of Conservation and Archaeology*. <https://doi.org/10.16334/j.cnki.cn31-1652/k.2005.04.004>
9. H.W. Liu, H. Wang, R. Zhang, L. Qu, Differentiation and research on the gold-red glaze for qing dynasty painted enamel. *Sci. Conserv. Archaeol.* **35**(05), 17–26 (2023)
10. C.S. Chari, Z.W. Taylor, A. Bezur, S.J. Xie, K.T. Faber, Nanoscale engineering of gold particles in 18th century Bottger lusters and glazes. *PNAS* (2022). <https://doi.org/10.1073/pnas.2120753119>
11. H. H. Lu, C. E. Cao, Y. X. Chen, W. Shi, X. L. Lu, X. L. Su, T. Zeng. 2020. *Journal of Ceramics*. **41**(03): 308–316
12. N.N.L. Dinh, L.T. DiPasquale, M.C. Leopold, R.H. Coppage, A multi-size study of gold nanoparticle degradation and reformation in ceramic glazes. *Gold Bull.* **51**(3), 75–83 (2018). <https://doi.org/10.1007/s13404-018-0230-7>
13. Fukang Zhang, the science of Chinese ancient ceramics. (Shanghai People's Fine Arts Publishing House, Shanghai, 2000, ISBN 978-7-5322-2516-X) p.111+165
14. B. Maheu, J.N. Letoulouzan, G. Gouesbet, Four-flux models to solve the scattering transfer equation in terms of Lorenz-Mie parameters. *Appl. Opt.* **23**(19), 3353–3362 (1984). <https://doi.org/10.1364/AO.23.003353>
15. B. Maheu, G. Gouesbet, Four-flux models to solve the scattering transfer equation: special cases. *Appl. Opt.* **25**(7), 1122–1128 (1986). <https://doi.org/10.1364/AO.25.001122>
16. P.A. Cuvelier, C. Andraud, D. Chaudanson, J. Lafait, Copper red glazes: a coating with two families of particles. *Appl. Phys. A* **106**(4), 915–929 (2011). <https://doi.org/10.1007/s00339-011-6707-3>
17. C. Mätzler, MATLAB Functions for Mie Scattering and Absorption. (2002)
18. P.B. Johnson, R.W. Christy, Optical constants of the noble metals. *Phys. Rev. B* **6**(12), 4370–4379 (1972). <https://doi.org/10.1103/PhysRevB.6.4370>
19. E. D. Palik, Handbook of Optical Constants of Solids. (Academic Press, 1998), p.760
20. E. D. Palik, Handbook of Optical Constants of Solids II. (Academic Press, 1998), p.770
21. CDGM GLASS CO., LTD, Optical Glass Data Sheet. (2022) <https://refractiveindex.info/download/data/2022/CDGM202206.pdf>
22. T. Pradell, R.S. Pavlov, P.C. Gutiérrez, A. Climent-Font, J. Molera, Composition, nanostructure, and optical properties of silver and silver-copper lusters. *J. Appl. Phys.* **112**, 054307 (2012). <https://doi.org/10.1063/1.4749790>

23. R.H. Lambertson, C.A. Lacy, S.D. Gillespie, M.C. Leopold, R.H. Coppage, Gold nanoparticle colorants as traditional ceramic glaze alternatives. *J. Am. Ceram. Soc.* **100**(9), 3943–3951 (2017). <https://doi.org/10.1111/jace.14928>
24. C.E. Cao, X.L. Lu, Y.X. Chen, H.R. Shen, C. Hong, F. Yu, Colouration mechanism of lead and arsenic free gold ruby famille-rose pigments. *J. Chinese Ceram. Soc.* **39**(11), 1734–1739 (2011)
25. Born, M. and E. Wolf, Principles of Optics (translated into Chinese by Jiasun Yang, ISBN 978–7–121–28932–3). (Publishing house of electronics industry, Beijing, 2016) pp.656–660

Springer Nature or its licensor (e.g. a society or other partner) holds exclusive rights to this article under a publishing agreement with the author(s) or other rightsholder(s); author self-archiving of the accepted manuscript version of this article is solely governed by the terms of such publishing agreement and applicable law.